Anticline growth by shortening during crustal exhumation of the Moroccan Atlantic margin

Fernández-Blanco, D.; Gouiza, M.; Charton, R.; Kluge, C.; Klaver, J.; Brautigam, K.; Bertotti, G.

DOI
10.1016/j.jsg.2020.104125

Publication date
2020

Document Version
Final published version

Published in
Journal of Structural Geology

Journal of Structural Geology 140 (2020) 104125

Contents lists available at ScienceDirect

Journal of Structural Geology

journal homepage: http://www.elsevier.com/locate/jsg

Anticline growth by shortening during crustal exhumation of the Moroccan Atlantic margin

D. Fernández-Blanco [a,*], M. Gouiza [b], R. Charton [a,e], C. Kluge [a], J. Klaver [c], K. Brautigam [d], G. Bertotti [a,e]

[a] TU Delft University, Faculty of Civil Engineering and Geosciences, Delft, Netherlands
[b] University of Leeds, School of Earth and Environment, Leeds, England, UK
[c] RWTH Aachen University, Structural Geology, Tectonics and Geomechanics, Aachen, Germany
[d] Vrije Universiteit Amsterdam, Tectonics and Structural Geology Department, Amsterdam, Netherlands
[e] North Africa Research Group (NARG), UK

A B S T R A C T

It is unclear how the crustal-scale erosional exhumation of continental domains of the Moroccan Atlantic margin and the excessive subsidence of its rifted domains affected the Late Jurassic-Early Cretaceous post-rift evolution of the margin. To constrain the km-scale exhumation, we study the structural evolution of the Jbel Amsittene. This anticline is located on the coastal plain of the Moroccan Atlantic margin, and is classically considered to have been developed initially in the Late Cretaceous by halokinesis, and by contraction during the Neogene. Contrarily, our structural analysis indicates that the anticline is a fault-propagation fold verging north with Triassic salts at its core and that it formed by shortening shortly after continental breakup of the Central Atlantic. The anticline grew by NNW-SSE to NNE-SSW contraction, as shown by syn-tectonic wedges, regional kinematic indicators and synsedimentary structures in Upper Jurassic to Lower Cretaceous rocks. It grew further and tightened during the Cenozoic, presumably in relation to the Atlas/Alpine contraction. Thus, our data and interpretation suggest that "tectonic-drives-salt" in the anticline early growth, which is coeval with the growth of other anticlines along the Moroccan Atlantic margin and widespread km-scale exhumation farther onshore. Anticline growth due to shortening argues for intraplate far-field stresses potentially linked to the geodynamic evolution of the African, American and European plates.

1. Introduction

The evolution of the Atlantic rifted margin in Morocco (Fig. 1) is marked by a period of atypically excessive subsidence during the Late Jurassic-Early Cretaceous (Gouiza, 2011; Bertotti and Gouiza, 2012). This early post-rift subsidence affected the distal deep basins, the continental shelf and the proximal coastal basins of the Atlantic margin, and was coeval with km-scale erosional exhumation of large continental domains to the east (Ghorbal et al., 2008; Ghorbal, 2009; Saddiqi et al., 2009; Oukassou et al., 2013; Leprêtre et al., 2015a; Gouiza et al., 2017). The underlying process behind this exhumation is still unclear, for it took place ~30–~50 My after lithospheric breakup between Morocco and Nova Scotia (Klitgord and Schouten, 1986; Sahabi et al., 2004) but prior to the Atlas/Alpine shortening that raised the Atlas and the Rif mountain belts (Frizon de Lamotte et al., 1991, 2008; Laville and Piqué, 1992).

Similarly to other passive continental margins with comparable movements of their hinterlands (Japsen and Chalmers, 2000; Japsen et al., 2006, 2009; Peulvast et al., 2008; Bonow et al., 2009), the anomalous vertical movements in Morocco are likely to be driven by tectonic processes. Mechanisms proposed for the Central Atlantic include long wavelength mantle processes (e.g., dynamic topography; e.g., Hoggard et al., 2016; Müller et al., 2018), surface processes (e.g., climate driven enhanced erosion; e.g., Westaway et al., 2009), regional tectonics (e.g., rift uplifted shoulder; e.g., Ruiz et al., 2011) and horizontal far-field stresses linked to rifting onset or mid-oceanic ridge spreading (e.g., Bertotti and Gouiza, 2012; Japsen et al., 2012; Green et al., 2018). Mantle processes alone, such as small-scale convection cells at the base of the mantle lithosphere may not be able to explain the crustal km-scale exhumation during the early post-rift (Gouiza, 2011). In this frame, attempts to link the Late Jurassic-Early Cretaceous exhumation in the east to the coeval subsidence in the west have overlooked the existence of contemporaneous NE-SW to NNE-SSW crustal shortening that might have driven both upward and downward vertical movements along the margin (Gouiza, 2011; Bertotti and Gouiza, 2012).

The Essaouira-Agadir Basin is located on the coastal plain of the

* Corresponding author. Current affiliation: Consejo Superior de Investigaciones Científicas (CSIC), Instituto de Ciencias del Mar (ICM), Passeig Marítim de la Barceloneta, 37-49, E-08003 Barcelona, Spain.
E-mail address: geo.david.fernandez@gmail.com (D. Fernández-Blanco).

https://doi.org/10.1016/j.jsg.2020.104125
Received 6 March 2020; Received in revised form 19 June 2020; Accepted 19 June 2020
Available online 30 June 2020

Atlantic rifted margin in Morocco, bounded to the E and NE by the Palaeozoic basement highs of the Massif Ancien of Marrakech and the Jebilets, respectively (Fig. 1). These massifs have experienced substantial exhumation in the early post-rift history (Middle-Late Jurassic to Early Cretaceous; e.g., Ghorbal et al., 2008; Ghorbal, 2009), while the Essaouira-Agadir Basin records clastic input in the Middle Jurassic and Early Cretaceous (Duval-Arnould, 2019; Luber et al., 2019). The Essaouira-Agadir Basin is thus an ideal location to investigate the tectonic processes responsible for the km-scale vertical movements (Fig. 1B). Most of the compressional structures observed in the

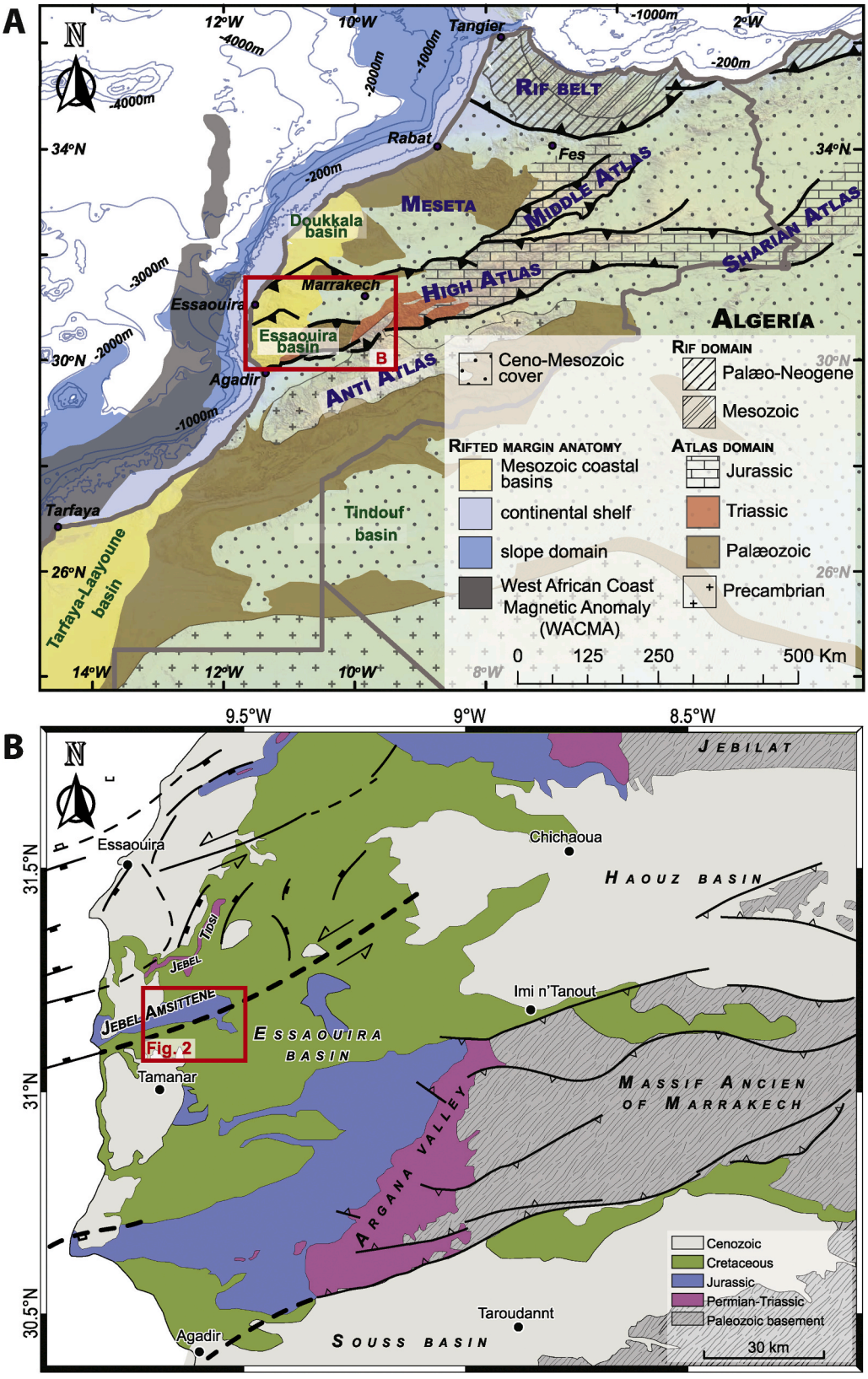

Fig. 1. Maps of tectonic provinces and geology. (A) Regional map of Morocco showing the major tectono-stratigraphic provinces and basins of coastal Western Morocco (simplified from the geological map of Morocco; Hollard et al., 1985). With indication of the location of Panel B. **(B)** Geological map of the western High Atlas and Essaouira-Agadir Basin showing the main Triassic-Liassic rift-related structures near the Jbel Amsittene Anticline (Hollard et al., 1985; Le Roy and Piqué, 2001).

Essaouira-Agadir Basin are attributed to Alpine shortening events leading to the uplift of the Atlas Belt (Hafid et al., 2006; Hafid, 2000; Ellouz et al., 2003). Thickness changes observed in Upper Jurassic to Upper Cretaceous rocks are interpreted as resulting from synsedimentary halokinesis (Hafid et al., 2006; Hafid, 2000). However, other studies show that numerous contractional structures developed during the Late Jurassic-Early Cretaceous in the western High Atlas and surroundings (Gouiza, 2011; Bertotti and Gouiza, 2012; Benvenuti et al., 2017).

The Jbel Amsittene Anticline is located in the central western part of the Essaouira-Agadir Basin and is one of several comparable structures, within the western High Atlas basins, thought to be formed by salt diapirism from the Late Cretaceous onwards (Piqué et al., 1998; Hafid, 2000; Le Roy and Piqué, 2001). In this work, we carry out a structural analysis of the Jbel Amsittene Anticline (Figs. 1B & 2), based on field observations in the Jurassic and Cretaceous rocks, and structural modeling. We present new evidence to discuss the tectonics of the formation of the Jbel Amsittene Anticline and its relationship with the growth of other structures in the context of regional vertical movements in the Moroccan rifted margin of the Central Atlantic.

2. Geological background

The Essaouira-Agadir Basin forms the western termination of the Moroccan High Atlas (Fig. 1). The basin evolved as part of the Atlantic rift during Triassic to Early Jurassic times and as a proximal shallow-water platform of the rifted margin since the Middle Jurassic (e.g., Hafid, 2000). Later convergence between Africa and Iberia/Europe since Late Cretaceous caused N–S to NNW-SSE regional shortening that inverted the Atlas rift, including the Essaouira-Agadir Basin, and built-up the Atlas Mountains (e.g., Hafid et al., 2006; Hafid, 2000; Piqué et al., 2002; Lanari et al., 2020a, 2020b). The basin is bounded to the south by lithospheric-scale faults that continue along-strike of the High Atlas belt, and is marked with transpressional and transtensional reactivations since the continental break-up (Ellero et al., 2020).

The Essaouira-Agadir Basin is composed of grabens and half-grabens bounded by N–S to NNE-SSW normal faults and E-W transform faults (Hafid et al., 2006; Hafid, 2000). These extensional rift structures are filled by terrigenous red beds of Triassic age with widespread intercalations of basalt flows, unconformably overlain by an early Lower Jurassic evaporitic sag basin (Hafid et al., 2006). An early Pliensbachian unconformity is commonly considered to be the breakup unconformity, and seals syn-rift sequences and structures (Medina, 1995). Following continental breakup in the Central Atlantic, sedimentation became mostly marine in the Essaouira-Agadir Basin, leading to accumulation of a thick carbonate platform in the Middle Jurassic to Lower Cretaceous (increasing westwards from 0.5 km to 2 km; e.g., Zühlke et al., 2004), with sandstone and shale interbeds. Deposition of Upper Cretaceous to Neogene shale-dominated series followed, with intercalations of limestone beds (Hafid, 2000). Shortening in the Atlas domain initiated in the Late Cretaceous, leading to the formation of the Atlas fold-and-thrust belt (Frizon de Lamotte et al., 2000; Piqué et al., 2002; Teixell et al., 2003), and is believed to have triggered the formation of salt-cored anticlines in the Essaouira-Agadir Basin, with minor inversion of Triassic normal faults (Hafid et al., 2006).

Other major tectonic events affected the Moroccan margin after the opening of the Central Atlantic Ocean in addition to the inversion and uplift of the Atlas belt (e.g. Teixell et al., 2003). Low-temperature thermochronology documents km-scale exhumation that affected most of the Precambrian-Palaeozoic domains exposed to the east of the Atlantic margin (i.e. Meseta plateau, Jebilet, Massif Ancien of Marrakech, Anti-Atlas belt) during Late Jurassic-Early Cretaceous times (Ghorbal et al., 2008; Ghorbal, 2009; Saddiqi et al., 2009; Ruiz et al., 2011; Oukassou et al., 2013; Sehrt, 2014). The Palaeozoic basement highs bounding the Essaouira-Agadir Basin, the Massif Ancien of Marrakech to the east, and the Jebilet to the northeast, experienced km-scale exhumation during the Late Jurassic-Early Cretaceous (Ghorbal, 2009; Saddiqi et al., 2009). Coeval exhumation events are also documented along the margin in the Meseta plateau to the north (Ghorbal, 2009; Saddiqi et al., 2009) and in the Anti-Atlas to the south (Malusà et al., 2007; Ruiz et al., 2011; Oukassou et al., 2013; Sehrt, 2014; Gouiza et al., 2017; Charton et al., 2018). This regional exhumation seems to have occurred during the post-rift stage of the Central Atlantic Ocean, i.e. ~30–~50 Myr after lithospheric breakup between Morocco and Nova Scotia (Klitgord and Schouten, 1986; Sahabi et al., 2004), and thus, before the Atlas/Alpine contraction that gave rise to the Atlas and the Rif mountain belts (Frizon de Lamotte et al., 1991, 2008; Laville and Piqué, 1992) and related km-scale exhumation (Lanari et al., 2020b).

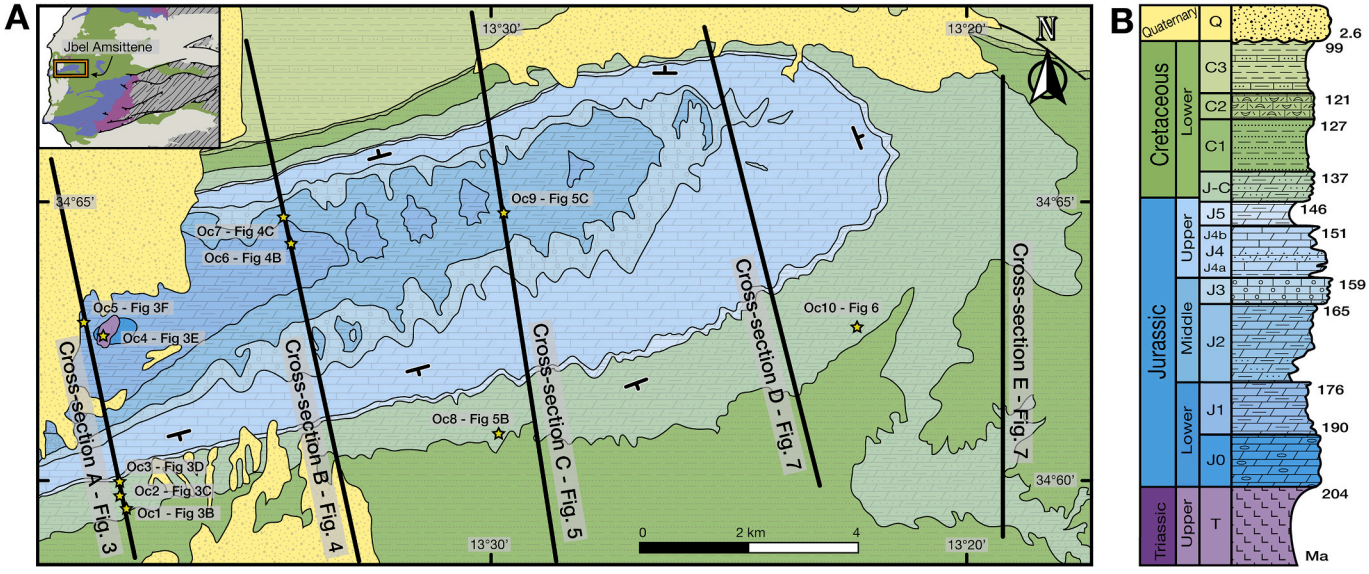

Fig. 2. Geology and chronostratigraphy in the Jbel Amsittene Anticline. (A) Geological map of the Jbel Amsittene Anticline, showing the location of the main observations in the field (yellow stars) and cross-sections that have been used to constrain the geological evolution of the area. Outcrops and outcrop numbers are shown as Oc.#. **(B)** Simplified chronostratigraphic and environmental column of the Jbel Amsittene area. Based on Hafid (2000), the geological map of Tamanar from the Moroccan Geological Survey and Zühlke et al. (2004). (For interpretation of the references to color in this figure legend, the reader is referred to the Web version of this article.)

Jbel Amsittene is a well-exposed salt-cored anticline that strikes ENE-WSW (Fig. 2A). It is located on the coastal plain of the W Moroccan Atlantic margin, in the northwest of the Essaouira-Agadir Basin between the cities of Essaouira to the north and Agadir to the south (Fig. 1). The Jbel Amsittene Anticline has a limited extent to the west where offshore seismic data shows no folding ~10 km off the present coastline (Hafid et al., 2006).

The stratigraphy of Jbel Amssittene used in this study is based on Duffaud et al. (1966), Jaïdi et al. (1970) and Zühlke et al. (2004). The stratigraphic column shown in Fig. 2B is taken from the 1:100000 geologic map of the study area (Jaïdi et al., 1970), and shows an almost-continuous series of Upper Triassic to Lower Cretaceous rocks unconformably covered, near the coast, by Quaternary sediments. The oldest formation, exposed in the core of the anticline, comprises Upper Triassic (T) terrigenous sandstones and evaporites. An erosional event, marked by a stratigraphic gap, occurred before Early Jurassic (J0-J1) open-marine deposition. A gradual transition from floodplain to inner shelf environment during the Middle Jurassic (J2-J3; e.g., Duval-Arnould, 2019), resulted in a sedimentary change from predominantly siliciclastic sand-dominated units to shallow marine carbonates. The Upper Jurassic (J4-J5) sediments are mainly shallow marine carbonates of inner shelf to lagoonal environment, although there are some sandstones and clastic interbeds (Ouajhain et al., 2011). An environmental change from inner (J/C–C1–C2) to outer shelf occurred by the end of the Early Cretaceous (C3). Quaternary terrestrial colluviums and coastal deposits overlie the Mesozoic rocks (Fig. 2).

3. Jbel Amsittene Anticline geological cross-sections and field observations

We performed detailed structural fieldwork to understand the tectonic history of the Jbel Amsittene Anticline. Whenever possible, we

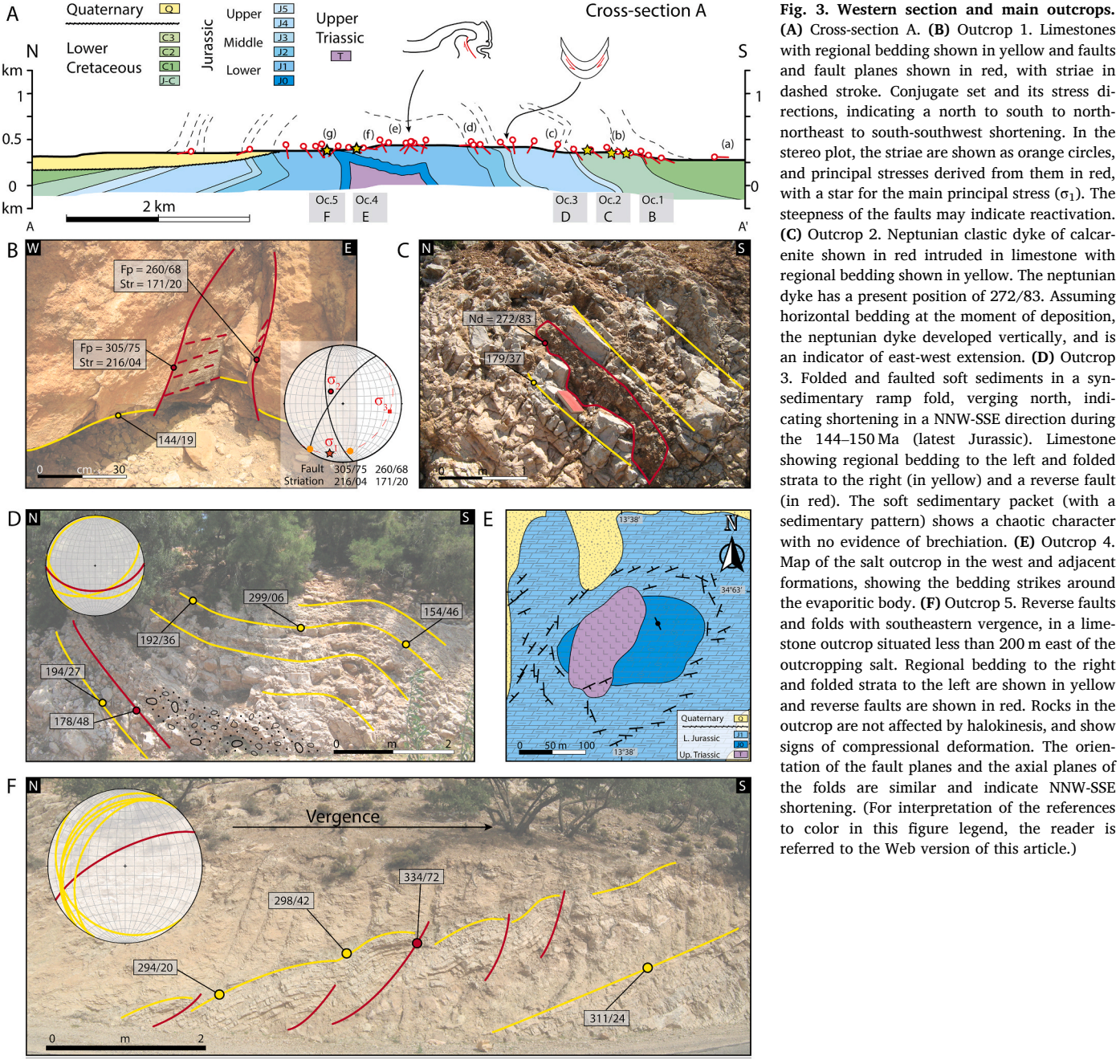

Fig. 3. Western section and main outcrops. **(A)** Cross-section A. **(B)** Outcrop 1. Limestones with regional bedding shown in yellow and faults and fault planes shown in red, with striae in dashed stroke. Conjugate set and its stress directions, indicating a north to south to north-northeast to south-southwest shortening. In the stereo plot, the striae are shown as orange circles, and principal stresses derived from them in red, with a star for the main principal stress (σ_1). The steepness of the faults may indicate reactivation. **(C)** Outcrop 2. Neptunian clastic dyke of calcarenite shown in red intruded in limestone with regional bedding shown in yellow. The neptunian dyke has a present position of 272/83. Assuming horizontal bedding at the moment of deposition, the neptunian dyke developed vertically, and is an indicator of east-west extension. **(D)** Outcrop 3. Folded and faulted soft sediments in a syn-sedimentary ramp fold, verging north, indicating shortening in a NNW-SSE direction during the 144–150 Ma (latest Jurassic). Limestone showing regional bedding to the left and folded strata to the right (in yellow) and a reverse fault (in red). The soft sedimentary packet (with a sedimentary pattern) shows a chaotic character with no evidence of brechiation. **(E)** Outcrop 4. Map of the salt outcrop in the west and adjacent formations, showing the bedding strikes around the evaporitic body. **(F)** Outcrop 5. Reverse faults and folds with southeastern vergence, in a limestone outcrop situated less than 200 m east of the outcropping salt. Regional bedding to the right and folded strata to the left are shown in yellow and reverse faults are shown in red. Rocks in the outcrop are not affected by halokinesis, and show signs of compressional deformation. The orientation of the fault planes and the axial planes of the folds are similar and indicate NNW-SSE shortening. (For interpretation of the references to color in this figure legend, the reader is referred to the Web version of this article.)

differentiated between two deformational events; (i) deformation related to Late Jurassic - Early Cretaceous structures involving soft sediment deposition, as a means to assess the stress field during the early post-rift of the Central Atlantic, and (ii) deformation related to (presumably-Cenozoic) Alpine events. We show relevant and representative outcrops (Fig. 2A) that summarize the main structural observations along three cross-sections. We provide uninterpreted pictures of these outcrops and complementary pictures in the Supplementary Material.

The studied geological cross sections are roughly 4 km apart transecting the anticline across its axis, NNW-SSE, and were constrained by bed measurements and field observations. Cross-section A (Fig. 3) is parallel to a road-cut for most of its length, which results in the best rock exposures in the area. Jurassic and Cretaceous rocks outcrop in the south and central parts of the section and are covered by Quaternary deposits in the northern region. Cross-section B (Fig. 4) is located ~4 km east of cross-section A and parallel to it. Cross-section B has sectors with poor accessibility or covered by vegetation and a small number of well-preserved outcrops. Cross-section C (Fig. 5) is ~4 km east of cross-section B, and parallel to the previous sections. We further detail two additional cross-sections and an outcrop farther east. Finally, we describe and recapitulate information relevant for the discussion in the form of along-strike and across-strike lateral variations, syn-sedimentary deformation, and a 3D thickness model.

3.1. Western section: Cross-section A

The lower Lower Cretaceous (C1) to lower Middle Jurassic (J2) limestone, marl, and sandstone layers dip south in most of the southern flank and change from horizontal to steeply north-dipping where the topography is the highest. North of the topographic high, layers dip south again and finally outcrop as overturned, prior to being covered by Quaternary deposits in the northernmost area of the section. Quaternary rocks prevent an unambiguous thickness comparison between the older units on both sides of the anticline. Those that could be compared showed no changes in thicknesses. The transition from horizontal to overturned layers is observed in the oldest Jurassic limestones and shales exposed in this section (lowermost Jurassic, J1). The dip of the stratigraphic layers indicates a northward verging anticline with a tête-plongeante (plunging head) shape (sensu Seguret, 1972) in its central-northern sectors.

Lower Cretaceous marls and carbonates dip gently to the south (10°-20°) in the southernmost part of the southern flank ("a" in Fig. 3A), and become steeper towards the north, reaching dips of ~80° at the highest point of the topography. Changes in dip are not constant and north dipping layers outcrop in the central sector of the southern flank (Fig. 3A), within the middle and lower Upper Jurassic shales, marls and limestones (J4). Moving northwards, the dip of the layers locally changes in relation to secondary N-verging folds tens of meters in size. Three conjugate fault sets outcrop in a local topographic flat (Fig. 3A), in the uppermost Upper Jurassic-lowermost Lower Cretaceous (J-C) limestones. We identify conjugate sets as faults with the same kinematics, coherent dip and dip angle (between ~45 and 60°), and independently-measured striae on both fault planes located at ~90° from the fault planes intersection, and derive the orientation of the stress ellipsoid from the striations of conjugate faults (Fig. 3B). We show one of them in Oc1 (Fig. 3B). The regional bedding dips gently to the SSE, and the three conjugate fault sets show clear striations of sub-horizontal to gently S directions (from 216°/04° to 171°/20°). The fault planes and associated striations are indicative of N–S to NNE-SSW maximum horizontal stresses, both for limestones rotated with respect to the regional bedding (post-tilted) and non rotated (pre-tilted). From this outcrop northwards, bed dips start to increase and reach values up to ~55° toward the south ("b"; Fig. 3A). Less than 50 m before the exposure of the lower Lower Cretaceous limestones and marls (C1), a N–S-striking sub-vertical clastic dyke of marine clastics cuts S-dipping strata (Oc2; Fig. 3C). A few meters northwards, a syn-sedimentary N-verging ramp fold indicates soft sediment deformation (Oc3; Fig. 3D). Whereas the conjugate fault set in Oc.1 (Fig. 3B) suggests no deformation took place before deposition of

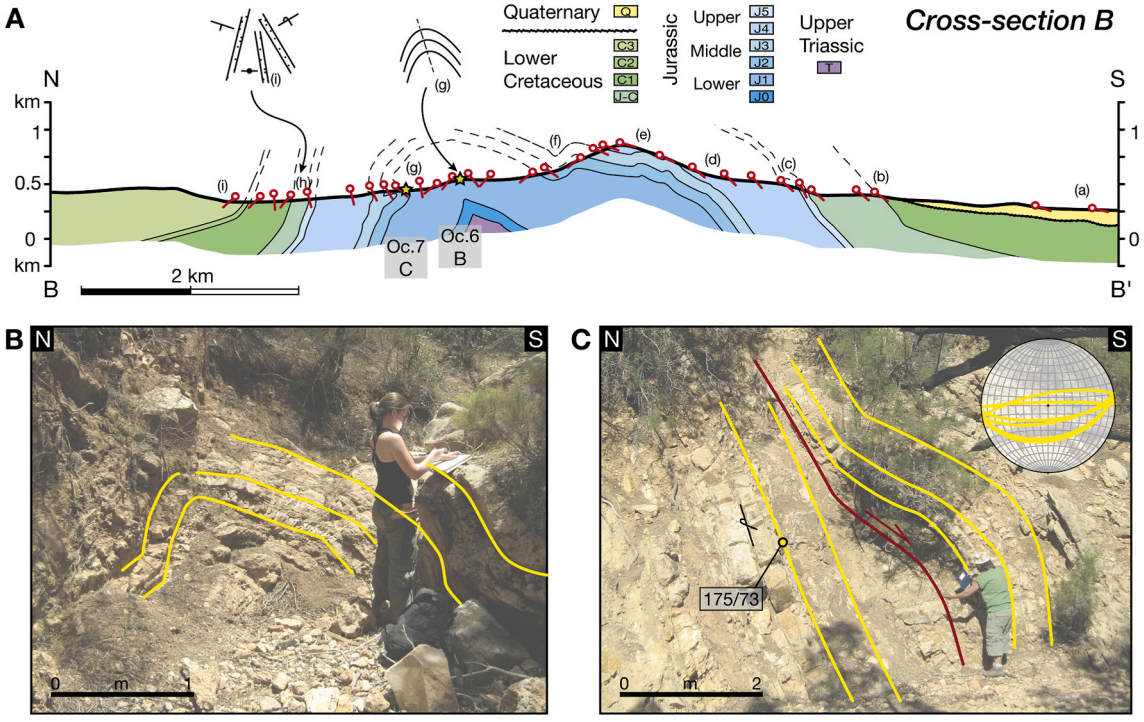

Fig. 4. Central section and main outcrops. (A) Cross-section B. **(B)** Outcrop 6. Meter-scale fold in limestones at the location of main dip change in beds (shown in yellow) at the anticline axis. **(C)** Outcrop 7. Underthrust in overturned limestone strata. The fault is in red and beds are in yellow. Fault-bend fold, with top to the south movement, with 175/73 regional bedding. The fold in the hanging wall has a fold axis of 085/06 and axial plane of 022/14. (For interpretation of the references to color in this figure legend, the reader is referred to the Web version of this article.)

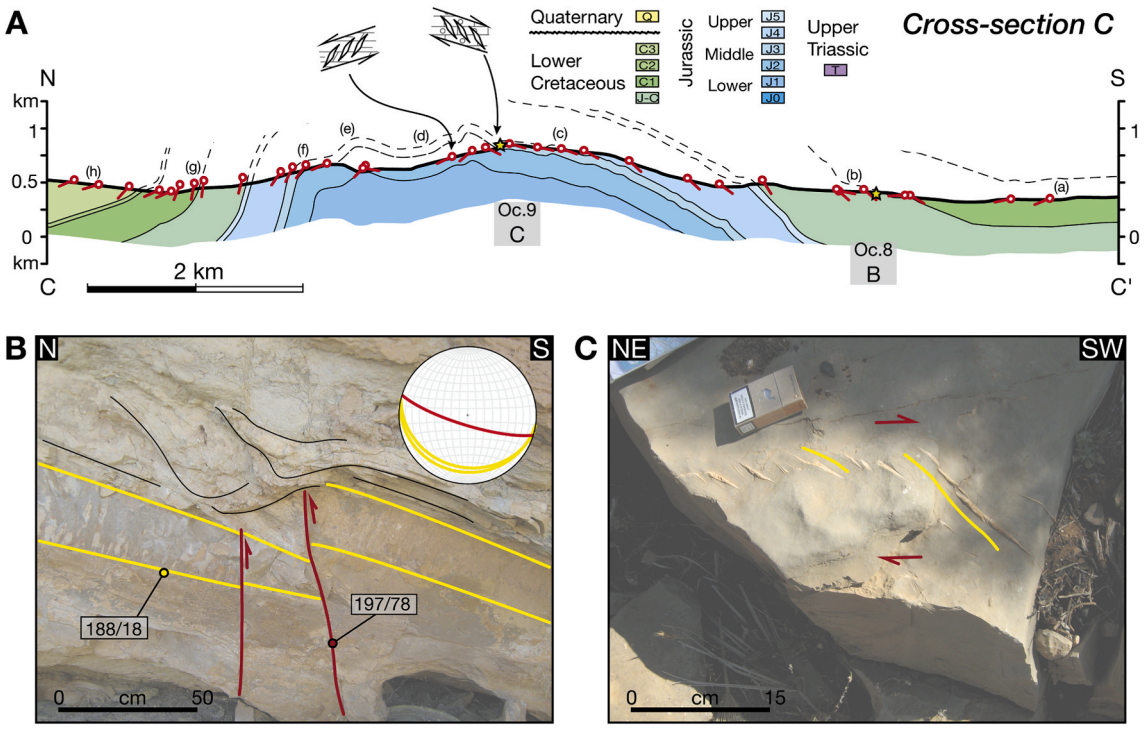

Fig. 5. Eastern section and main outcrops. (A) Cross-section C. **(B)** Outcrop 8. Inclined limestone layers cut by synsedimentary faults. High-angle reverse faults (in red) transect a thick bank (with its top and its bottom beds in yellow) with an offset of ~20 cm. The reverse fault tips end in the sedimentary layer on top that show soft sediment deformation of chaotic nature (in thin black), bracketing the age of deformation to 146-137 Ma (J-C formation, lowermost Lower Cretaceous – uppermost Lower Jurassic). The inclination of the reverse faults is suggestive of reactivation of former normal faults. **(C)** Outcrop 9. One of the two sets of sigmoidal tension gashes that outcrop at both sides of one of the anticline axes, in limestones. They indicate right lateral shear. (For interpretation of the references to color in this figure legend, the reader is referred to the Web version of this article.)

uppermost Upper Jurassic – lowermost Lower Cretaceous unit (J-C), the latter two syn-sedimentary structures (Oc2; Oc3, Fig. 3C and D) indicate NNW-SSE shortening during its deposition.

Structures north of these outcrops seem to be exclusively related with the Alpine deformation phase. Approximately 200 m north of these outcrops, the Upper Jurassic shale and limestone layers (J5) dip north ("c" in Fig. 3A). Steep and sub-vertical N-dipping overturned layers alternate occasionally with S dipping beds ("d") for ~400 m in lower and middle Upper Jurassic rocks (J4). Bedding-parallel flexural slip associated with Alpine deformation is common and related striations show a N–S slip direction. Northward, Middle Jurassic (J3-J2) limestones and fine clastics dip consistently south until the topographic profile reaches its highest elevations ("e"). North of the topographic high, the orientation of Lower Jurassic strata (J1) changes from subvertical (~80°) to subhorizontal with a gentle S-dip within a distance of ca. 500 m (Fig. 3A). Between the sub-vertical and sub-horizontal Lower Jurassic (J1) layers, S and N dipping sub-vertical strata alternate. Within this sector ("f" in Fig. 3A), highly deformed structures appear, showing faulted and folded strata, m-folds, recumbent folds, fault-related-folds, and more complex features, with unclear or non-sequential vergence. More to the north, the Lower Jurassic dolomites show no consistent strike for ~300 m, and layers are overturned (up to ~60°) or S-dipping. Around 300 m east of the section, Upper Triassic evaporites (T) outcrop in a circular depression of approximately 1 km in diameter (Oc.4; Fig. 3E). An intrusive contact is seen between the evaporites and the lowermost Jurassic unit (J1). The Lower Jurassic bedding dips away from the outcropping evaporites, from sub-vertical nearby to 25° in a few hundred meters farther away from them. The strike directions of these Jurassic rocks vary consistently around the salt, in an overall concentric configuration. The strike directions progressively change to the regional E–W to SW–NE trends 300–400 m away from the evaporites. Continuing north along cross-section A, overturned strata become subvertical (80°-85°) ("g") and finally N-dipping, before reaching the sub-horizontal Quaternary (Q) rocks that unconformably cover most of the northern flank. In this area, a sequence of SSE-verging fault-propagation folds outcrops in the Lower Jurassic limestones (J1), with axial planes indicating a SSE-to-NNW shortening direction (Oc5; Fig. 3F).

3.2. Central section: Cross-section B

Gently south dipping lower Middle Jurassic (J2) to lower Lower Cretaceous (C1) shales and limestones outcrop from the southern side of the anticline until significantly north of the topographic high (Fig. 4A). The oldest rocks seen in the section are Lower Jurassic (J1; shales) and outcrop ~1,5 km north of the topographic high, in the core of the anticline. North of the hinge of the anticline there are steep north dipping layers of lower Middle Jurassic (J2) to Lower Cretaceous (C1) age. Some of these steep layers are overturned and dip south ("i" in Fig. 4A). Further north, the Lower Cretaceous strata (C2–C3) have gentle north dipping slopes. The uppermost Upper Jurassic to lower Lower Cretaceous (J-C to C1) rocks are significantly thinner in the northern (~350 m) than in the southern (>900 m) flank along cross-section B (Fig. 4A).

In the southernmost of cross-section B, Quaternary (Q) deposits cover Lower Cretaceous rocks (C1–C3) ("a" in Fig. 4A). Northwards, rocks of the uppermost Upper Jurassic to lower Lower Cretaceous (J-C to C1) outcrop with consistent dips of ~40° to the south ("b"). Upper Jurassic (J4-J5) limestone layers have steeper dips that vary from ~40° to ~65° to the south ("c"). Further north, the Middle Jurassic (J2-J3) layers gradually decrease in steepness from ~45° to ~35° to the south ("d") and become roughly parallel to the topography ("e", dips of 10°–20° to the south) as they reach the topographic high.

Starting 300 m northwards of the topographic high, ~20°–40° south dipping layers alternate with ~40° north dipping layers. This trend

continues for ~400 m, and is seen also for parts of the Lower Jurassic (J1) rocks ("f"). Layers are folded asymmetrically in this area until the northward dips become dominant (Oc.6; Fig. 4B). Advancing farther north, these Lower Jurassic (J1) shale-limestone layers overturn and dip south again, for a distance of more than 900 m. Dip angles of overturned Lower Middle Jurassic (J2) layers are here less verticalized than along the rest of this section (175°/73°) ("g"). The Jurassic rocks are locally underthrusted in a fault-bend fold structure that indicates top to the south motion (Oc.7; Fig. 4C). The layers remain sub-vertical for around 1100 m, and gradually decrease in steepness, from ~85° to ~50° to the north, in the lowermost Cretaceous (J-C) unit ("h"). Toward the north, layers of the lowest Lower Cretaceous (C1) are sub-vertical again, while the middle Lower Cretaceous (C2) strata have shallower dips (40° N) ("i") that decrease gradually to 20° N when reaching the upper Lower Cretaceous (C3) shales. Observations show no evidence of synsedimentary deformation in the limestones and marls of uppermost Upper Jurassic to lower Lower Cretaceous (J-C to C1) age along the cross-section B, but these units show a decrease of >500 m in thickness across the anticline strike (Fig. 4A).

3.3. Eastern section: Cross-section C

Cross-section C portrays a north vergent anticline with two hinges, showing a northern steeply dipping flank and a southern gently dipping flank (Fig. 5A). The rocks exposed along this easternmost section are early Middle Jurassic (J2) to late Early Cretaceous (C3) in age. The thickness of the lowermost Cretaceous (J-C) formation varies from approximately 550 m on the southern flank to 400 m on the northern flank of the anticline, whereas the thicknesses of the Jurassic formations J2 to J5 are constant along the section.

In cross-section C, the southern flank of the Jbel Amsittene Anticline is characterized by south dipping sedimentary limestones, marls and shales ("a" in Fig. 5A), with subhorizontal Cretaceous rocks in its southernmost sector. Towards the north, older south-dipping carbonates crop out. Within the lowermost Lower Cretaceous – uppermost Lower Jurassic formation (J-C), layer inclinations vary between approximately 30° and 80° to the south ("b"). Here, the layers are locally offset by cm to dm-scale reverse faults, which indicate N–S to NNE-SSW shortening coveal with sedimentation. Outcrop 8 (Fig. 5B) shows an example of these reverse faults in limestones. SSW dipping faults in this outcrop have up to ~20 cm offset and terminate in the slumped overlying sediments that show soft deformation, indicating a possible phase of syn-sedimentary deformation during the early post-rift of the Central Atlantic.

Outcrops farther north evidence deformation due to Alpine shortening. Towards the topographic high, the dip of the bedding gradually decreases from ~40° to 20° to the south, and upper Middle to middle Upper Jurassic (J3 – J4) rocks are exposed ("c"). Calcite-filled tension gashes are observed in several outcrops in and around the topographic high (Oc. 9; Fig. 5C). The veins are spaced by a few cm, and show both top-to-the-north and top-to-the-south shear kinematics. The former occurs mostly to the south of the topographic high, and the latter is observed mainly to the north of the topographic high. Northwards, along a ~500 m sector, the beds are subhorizontal gently dipping to the north ("d"). Approximately 1 km farther north, beds dip to the south for ~100 m before dipping north again ("e") and lower Middle Jurassic (J2) carbonates and sandstones are exposed. In the second topographic high, where the second hinge plane of the anticline intersects the topography, the orientation of the bedding is 65° to the north ("f"). Between the second topographic high and the valley north of the Jbel Amsittene Anticline, successive upper Middle Jurassic (J3) to lower Lower Cretaceous (C1) strata are exposed steeply dipping north (60–80°) ("g"). North of the valley, Lower Cretaceous (C1 to C3) limestone and marl strata are exposed dipping ~10–20° northwards ("h").

3.4. Eastern sectors of the Jbel Amsittene Anticline

Other relevant structural observations were found eastwards of the above-described sections. The most relevant structure for the scope of this study outcrops ~5 km to the east of cross-section C, in the lowermost Cretaceous (J-C) limestones (Oc. 10; Fig. 6). This outcrop depicts a series of high angle reverse faults dipping SSW that transect limestones below a ~30 m long sedimentary wedge that pinches out towards the S. The top-to-the-north faults show reverse offsets of few to tens of centimeters and slickenlines indicating SSW-NNE shortening direction. The upper terminations of the faults are within the overlying lowermost Cretaceous syn-tectonic strata, and indicate active deformation during this period.

3.5. Structure and lateral variations in the Jbel Amsittene Anticline

We produced a structural map of the Jbel Amsittene (Fig. 7A). The map uses data collected from Section A to the coast, as in Brautigam et al. (2009), and two sections we reconstructed further east, where the anticline is more open (shown in Fig. 7B). These sections are similar in overall structure and geometry and change relevantly, albeit continuously, along the strike of the anticline (Fig. 7). The eastern sections (bottom of Fig. 7B) depict an open and asymmetrical anticline with a gentle north vergence. In the eastern sections (i) the southern limb dips gently and persistently south, (ii) salt deformation is not noticeable, neither in the hinge nor elsewhere, and (iii) the northern limb shows north dips with no overturned strata. The anticline shows a well-confined hinge and its flanks dip more gently than their western continuations. Small-scale structures are rare and more open. The layers along the limbs have an alternation of sectors with constant dip and sectors where dips vary progressively. By contrast, the western sections (top of Fig. 7B) present a tight structure and a clear north vergence. In the western sections, (i) the southern limb of the anticline dips south, from gently to steep, with local dips to the north, (ii) distortion by diapirism is limited to the vicinity of the hinge where the salt is outcropping, and (iii) the northern limb is frequently overturned and partly covered by Quaternary deposits. The western sections show a topographic crest characterized by a north tête-plongeante geometry. Strain markers are numerous and strata often show relevant changes in dip direction over short horizontal distances.

3.6. Thickness changes along the Jbel Amsittene

To obtain thickness variations in the Jurassic formation, we put forward a 3D thickness model integrating remote sensing (horizon mapping) and structural data (dip data and geological cross sections; Fig. 8). We used a "3 point-solver" plug-in for Google Earth™ to derive bed attitude from the contact between beds and topography at three or more points (Bennison and Moseley, 2003). With these means, we collect dip data of bed contacts tens of meters in scale, at various locations around the anticline. We mapped horizons on DEM-coupled satellite images (Google Earth Pro™) to obtain spatial coordinates of well-exposed geological contacts, identified by the georeferenced geological map of Choubert (1965) and color changes in the imagery. We used the mapped horizons and the large-scale (tens of meters) dip data in geological cross-sections to derive a 3D model of continuous stratigraphic surfaces using *StructuralLab* tool of *Gocad*. We then used the *kine3d-1* tool and *Matlab* to obtain true thickness maps from the mapped horizons. Model resolution suggests a precision of ~20 m at the surface, and hence lies below the thinnest stratigraphic units within the study area.

Thickness maps reveal an along-strike change in the thickness of Jurassic rocks (Fig. 8). Thickness variations comprise the Lower Jurassic (J0, J1), Middle Jurassic (J2, J3), and Upper Jurassic (J4, J5) along a clockwise profile from the northwestern to the southwestern fold flanks. We find maximum unit thicknesses in the overturned northern flank and

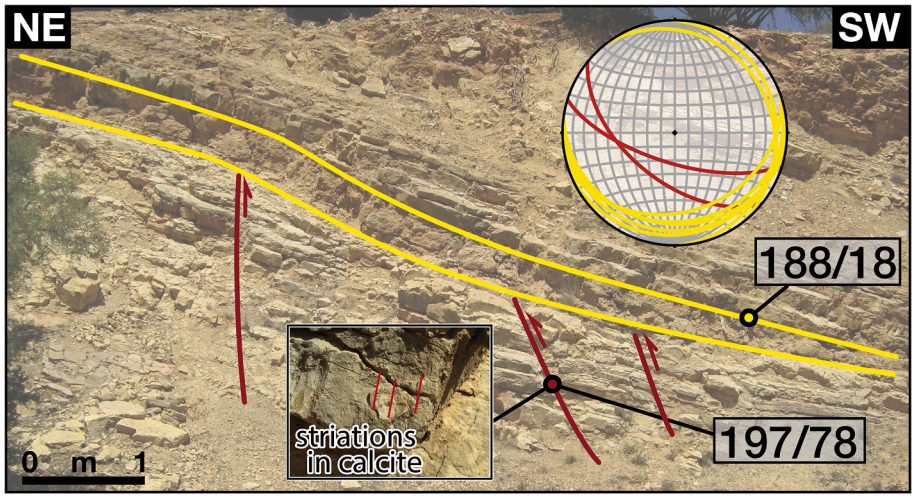

Fig. 6. Outcrop 10. Limestone outcrop showing an approximately 30 m long wedge pinching out towards the south, overlaying faulted strata. The top to the north-northeast faults have reverse offsets of a few to tens of centimetres that do not continue into the wedge, indicating a shortening direction of SSW-NNE during the J-C formation, uppermost Jurassic – lowermost Cretaceous. The steepness of the faults may be indicative of reactivation.

a decrease in thicknesses eastwards. Such thickness decrease is substantial at the point where the fold limbs change into NNW dipping beds. All formations follow this trend, that becomes less significant towards the Upper Jurassic (J4, J5). It is worth noticing, however, that modeling is less precise in overturned layers. In the southern limbs, towards the west, thicknesses in all formations increase progressively, albeit remaining below thicknesses of the northern limb (Fig. 8). Generally, thicknesses are never constant along the anticline strike for >5 km. Thickness at the eastern side are around 40–50 m in J3 and 140 m and 80 m in J4, respectively. Sediments increase in thickness towards the southern limbs, with 140 m–200 m for J3. This corresponds to a thickness increase of ~70–75%. The J4a (Oxfordian) strongly increases from around 140 m to more than 300 m.

We also derive thicknesses for the upper Upper Jurassic - Lower Cretaceous units (J-C, C1, and C2) using bed attitudes along unit contacts. We use this input to infer the planes of contact between the sedimentary units and calculate true thicknesses by measuring the distance between contacts orthogonally. Although this approach is less accurate and lacks the along-strike coverage of the aforementioned thickness model, it provides a valid first-order estimate on the variation of sedimentary thickness across strike. The upper Upper Jurassic - Lower Cretaceous units (J-C, C1, and C2) decrease in thickness northwards across the strike of the Jbel Amsittene Anticline (Table 1). As seen in cross-sections A and B (Figs. 4 and 5), formations J-C and C1 are up to ~350 m thinner in the northern flank with respect to the southern flank of the anticline (Table 1). These values represent a minimum estimate, given that the upper boundary of C1 is in places outside the limits of our study area. Our observations suggest that sedimentary thickness changes affect C2 as well, and that no thickness changes affect the Lower Cretaceous C3 formation. These thickness variations are less obvious in the east of the study area (Fig. 7).

4. Discussion

4.1. Key characteristics of the Jbel Amsittene Anticline

The Jbel Amsittene Anticline has a limited lateral extent and shows geometry changes along strike (Fig. 7). In the west, the anticline manifests as a box anticline with a gentle north vergence within a broader area of deformation. The anticline continues westwards for less than ~10 km off the coastline (Hafid, 2006). The tight tête-plongeante that the anticline has in the west smoothens and widens eastward into an open fold (up to ~20 km in wavelength) and eventually wanes. The eastward plunge of the fold axis and the southward dip of its axial plane (Fig. 7) results in the exposure of the oldest rocks at the core of the anticline in the west and their location to the north of the topographic high.

Thickness variations have different trends in Jurassic and Early Cretaceous units. Jurassic units show a signal of eastward decreasing thicknesses along strike, with maxima in the anticline center (Fig. 8). The cumulative thickness for the Jurassic units has sharp variations of up to 900 m between the northern flank and the eastern termination of the anticline, while between the latter and the southern flank, thickness variations are of ~600 m. A second-order signal across the anticline strike portrays a decrease in thickness towards the southern flank (Fig. 8). The combined thickness of units J-C and C1 decreases by up to 500 m northwardsacross the axis of the anticline, and by up to 250 m eastwards over a short distance (Table 1). Whereas thickness changes in Jurassic units seem unrelated to a tectonic event, the latter units may relate to changes in shortening rates, as shown below.

Differential strain distribution along the anticline strike can be inferred for modern and antecedent forms of the anticline. We derive along-strike changes in amount of shortening from variations in line-length approximations along the present anticline strike, and from the number and size of outcrop-scale syn-sedimentary structures in the Upper Jurassic – lower Lower Cretaceous (J-C) formation (Table 2). The western section presents line-length shortening values of ~1,6 km over a measured length of ~7,6 km, i.e., ~21% shortening. This shortening value remains almost constant in the central section (~20%), and decreases in the eastern section (14,5%). Farther east, in the easternmost section, we measured 0,2 km of shortening over a length of ~4,3 km, i.e. ~4,5% shortening (Table 2). Thus, line-length shortening decays along the Jbel Amsittene Anticline strike from its center to the east. Although most deformation and probably the observed eastward decay in shortening along the anticline strike relates to structure tightening during Alpine times, we infer a similar trend for the syn-depositional structures in the Upper Jurassic – lower Lower Cretaceous (J-C) formation. Most of such syn-depositional structures appear in the west of the anticline and are absent in coveal rocks in the east and in rocks of upper Lower Cretaceous (C3) age exposed in the northern part of the study area. This suggests that the eastwards decrease in shortening resulted in a westward-opening conical anticline by the end of the Lower Cretaceous (C3).

Syn-sedimentary deformation is common in outcrops of the uppermost Upper Jurassic-lowermost Cretaceous limestones (J-C), and is expressed as clastic dykes, fault-related folds and reverse faults affecting

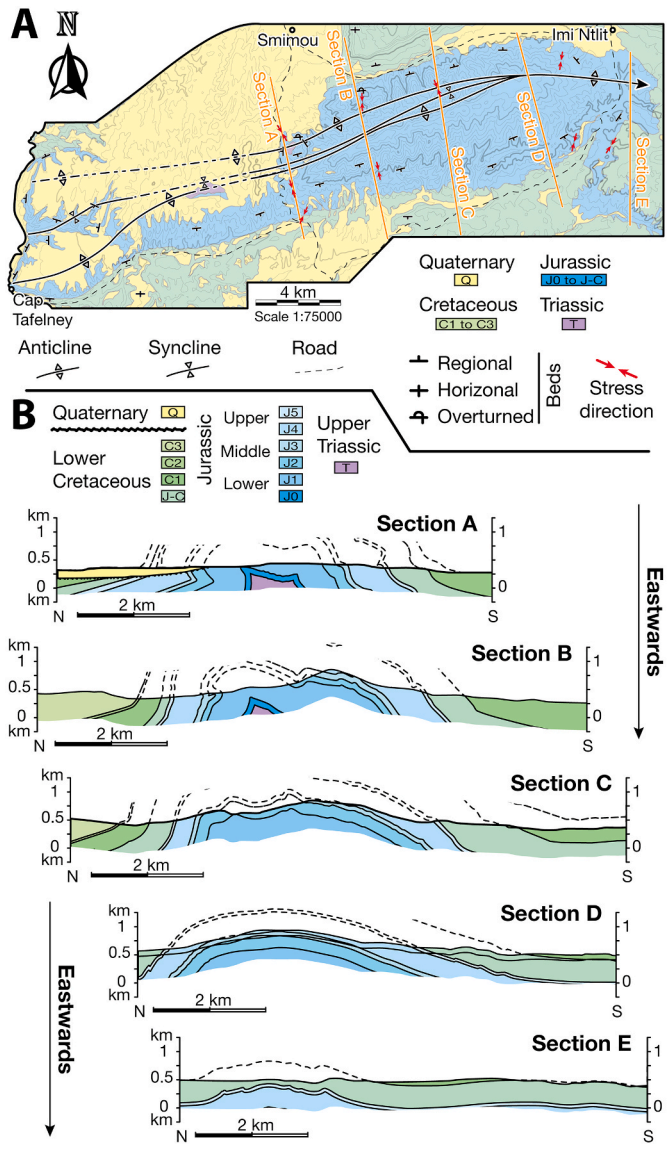

Fig. 7. Structure of the Jbel Amsittene Anticline. (A) Structural map showing the main axis of the anticline, its westward bifurcation, and its plunge towards the east. The map also shows regional bedding dips in different sectors of the anticline. The full bedding dip data collected in the fieldwork are provided in the Multimedia Component 3. Contours in grey represent lines of equal height every 50 m, with darker tones and thicker strokes for the heights of 250 m, 500 m and 750 m. **(B)** Geological sections in the Jbel Amsittene Anticline, from west to east, showing the anticline structure and vergence and its lateral variations.

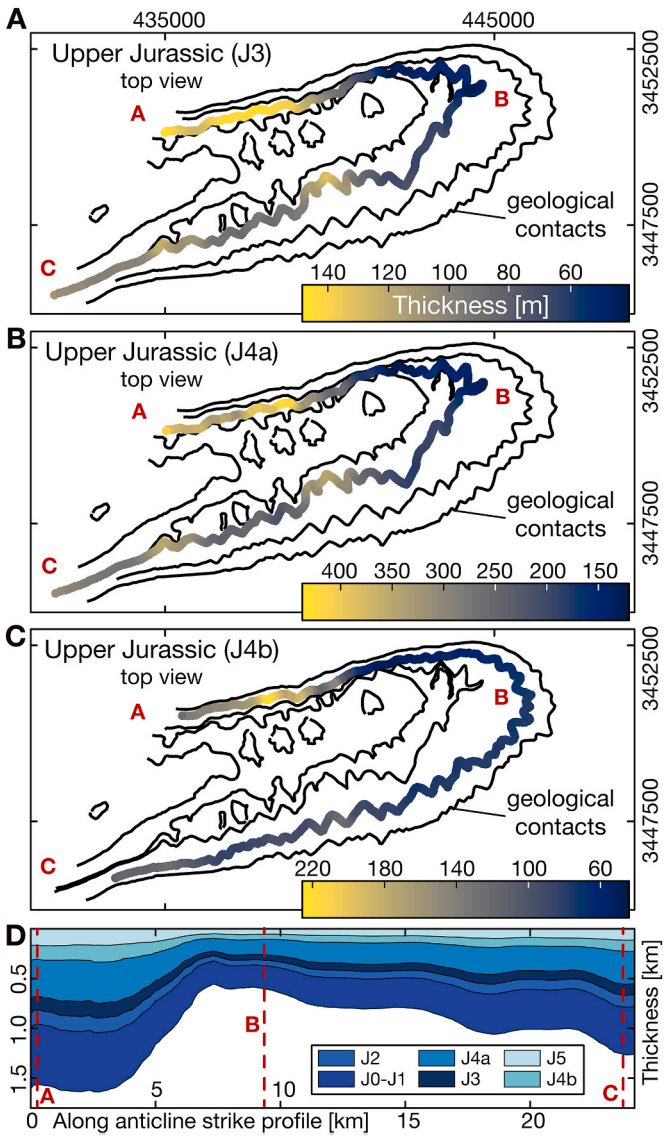

Fig. 8. Thickness model. (A/B/C) Model of thickness variations along contour likes of three Upper Jurassic sequences. (D) Modelled thickness variations of Jurassic rocks in a clockwise profile from the northwestern to the southwestern flank of the anticline.

soft sediment (Figs. 3–5, 7). Overall top-to-the-north steep reverse faults with tips that offset soft sediments by few to tens of centimeters (Figs. 5 and 6) suggest N–S to NNE-SSW shortening. This observation can be coupled with striae in nearby conjugate fault sets indicating NNW-SSE to NNE-SSW maximum horizontal stresses (Fig. 6). Other equivalent coeval reverse faults are also steep in their pre-rotated stages, and probably result from reactivation of Triassic–Liassic normal faults. Similar evidence of syn-sedimentary shortening during deposition of the J-C unit can be found along the anticline strike. However, regional layer dips for this unit vary greatly (between approximately 30° and 80°), and evidence in other outcrops, such as the tête-plongeante or the overturned strata, are clear indications of younger shortening. Taken together, the data suggest that shortening initiated anticline growth of the Jbel Amsittene during the early post-rift phase of the Central Atlantic, and

Table 1
Thickness changes between the northern and the southern flank of the Jbel Amsittene Anticline for formations J-C and C1.

	Formation J-C		Formation C1	
	N flank	S flank	N flank	S flank
Cross-section B	150 m	500 m	350 m	500 m
Cross-section C	400 m	650 m	350 m	450 m

Table 2
Decrease in amount of shortening to the east, measured as unfolded line-length.

	Deformed length (km)	Shortening (km)
Cross-section A	7,6	1,6
Cross-section B	9,5	2,1
Cross-section C	10,3	1,5
Cross-section D	9,1	0,6
Cross-section E	4,3	0,2

that the anticline further developed and tightened during the Alpine orogeny (e.g., Saura et al., 2013 in the Central High Atlas; Pichel et al., 2019b in the offshore Essaouira-Agadir Basin; this study in the Jbel Amsittene).

4.2. Models for the evolution of the Jbel Amsittene Anticline

We put forward two potential models for the evolution of the Jbel Amsittene Anticline in Mesozoic times. We discuss, on the basis of the evidence presented in this contribution, our preferred model for an initial Mesozoic anticline development, which was enhanced and partly overprinted in the Cenozoic. Comparative, detailed structural studies inclusive of similar onshore anticlines in the area are required to confidently discriminate among these two potential evolutionary models proposed for the Jbel Amsittene Anticline, and elucidate the underlying growth mechanism for equivalent structures in the Moroccan margin. Discrimination among different the models would have implications on the geodynamic causes controlling the anomalous vertical motions during the early post-rift phase along the African margin.

In the first scenario, we assume the diapiric rise of the Triassic salt at the core of the present anticline is the driving force leading anticline growth already during the Early to Middle Jurassic. Halokinesis and salt tectonics are well expressed in the area (Hafid et al., 2006; Hafid, 2000) and proposed to happen during this period in the Central High-Atlas (Saura et al., 2013) and in the offshore Essaouira-Agadir Basin (Pichel et al., 2019a). Although extensive diapirism exists offshore Morocco, no clear interpretations of pre-Cretaceous timing and mechanism(s) of salt mobilisation are available, and it thus may occur in relation to different mechanisms than in the onshore (Neumaier et al., 2016). Moreover, salt mobilisation may potentially lead to syn-sedimentary deformation along the sides of the diapir and sedimentary dykes (Morley et al., 1998; Giles and Lawton, 2002 respectively; see examples in Poprawski et al., 2014). The Late Jurassic-Early Cretaceous deformation features may therefore be gravity-driven sedimentation features of local origin that can form on any submarine slope of a few degrees.

Many syn-sedimentary faults observed in the field are very steep. This might be the result of fault measurements concentrating on the steep, upper tips of the faults, for none of the faults has its root exposed. Moreover, the upper tips seem to show a sharp termination, potentially lithology-controlled. Is it thus possible that these faults are intraformational, and that they, and folded units, were generated by shear stresses of individual sedimentary packages sliding along bedding planes. This could be associated with slope gravity processes or a rising salt diapir, but this is unlikely given that some of these structures have vergence towards the diapir. Slope oversteepening can be purely sedimentary, and tectonic processes do not have to be involved to explain their formation. In this scenario, vertical movements (Stets, 1992; Bertotti and Gouiza, 2012; Gouiza et al., 2017) could be linked to anticline fold growth and salt tectonics, such that a gravitational load is applied by the uplift of the High Atlas and by the subsiding continental margin, creating a hydraulic head and leading to salt activation (Pichel et al., 2019a). The presence of salt in the anticline core and Jurassic thickness variations along the anticline that do not relate to the present structure are potential indicators for such salt-driven scenario, although further evidence from nearby anticlines need to be found.

In the second scenario, we assume that the Jbel Amsittene Anticline initially formed by horizontal shortening in the latest Jurassic and earliest Cretaceous. Horizontal shortening would mark an initial period of contraction and folding during the early post-rift phase, leading to the syn-tectonic growth of sedimentary wedges at anticline and outcrop scales (Figs. 4 and 5). Shortening would have started during latest Jurassic – earliest Cretaceous (J-C) and continued during the deposition of the Lower Cretaceous unit (C1), but ended before unit C3 deposition. During this time, the Jbel Amsittene developed as an open anticline that was probably asymmetrical along strike. The Triassic salt would function as a weak detachment facilitating accommodation of the horizontal stresses that lead to the reactivation of pre-existing structures (e.g., basement rift-related faults) and initial anticline growth before Cretaceous-Cenozoic tectonics (Hafid et al., 2006; Tari et al., 2003; Hafid, 2006). This shortening tectonics would be consistent with field observations of syn-sedimentary structures in the J-C unit and structures with clear vergence tens of meters away from the outcropping salt (Fig. 3). The lack of coherency in trend or scale of the salt with the overall anticline structure are also indicators of absence of halokinesis in the Jbel Amsittene during early post-rift of the Central Atlantic. These observations imply that Triassic salts were mobilised during compression led by horizontal tectonic forces, and that the growth of associated structures occurred in relation to a blind thrust rooted in the Triassic salt. The tête-plongeante structure towards the west and overturned layers at some sites indicate further shortening and anticline tightening during Alpine times. These structures and their consistent change along strike (Fig. 7) argue for vertical anticline growth during two overprinting phases of shortening, both acting roughly in the N–S direction. We thus consider that the evidence reported here favors the second scenario by which the latest Jurassic – earliest Cretaceous growth of the Jbel Amsittene occurred by tectonic shortening.

The Jbel Amsittene Anticline ENE-WSW strike is parallel to the strike of the major structures bounding the High Atlas belt (Fig. 1B). These structures activated under a transtensional regime during the Triassic-Early Jurassic rifting of the Central Atlantic, and defined several pull-apart basins where grabens and half-grabens, bounded by N- to NE-trending normal faults, were filled by terrigenous and evaporitic deposits (Piqué et al., 2002; Laville et al., 2004; Frizon de Lamotte, 2005). In our attempt to reconstruct the evolution of the Jbel Amsittene through time, we hypothesize that the Jbel Amsittene Anticline formed in strata overlying a previous half-graben structure bounded by an E-dipping normal fault to the east and an E-W left-lateral strike slip fault to the north (Figs. 1B & 9). The latter is shown in the Mesozoic structural map of the Essaouira-Agadir Basin by Le Roy and Piqué (2001), based on seismic data. The presence and relative accommodation space expected from both these pre-existing structures could explain increasing Jurassic thicknesses westwards and northwards along and across anticline strike, respectively (Figs. 7 and 8). We interpret the upwards decreasing thickness in Upper Jurassic units (Fig. 9) as an indication that the aforementioned faults were sealed, at the latest, by the end of the Late Jurassic (rifting kinematics, for both High Atlas and Central Atlantic, end in the Early Jurassic; e.g., Michard et al., 2008). Subsequent Late Jurassic-Early Cretaceous folding of the Jbel Amsittene Anticline may have occurred by reactivation of the E-W structure as a blind thrust, as interpreted on the structural map of Hafid et al. (2006) and on their seismic interpretation. This would result in thicknesses that increase towards the hanging-wall, i.e. southwards across the anticline, and are thus opposite in trend with regards to those in the Jurassic units, in agreement with our data (Table 1). Such blind thrust would be rooted in Triassic evaporites, acting as a weak decollement layer between the basement and the overlying Mesozoic basin infill (Fig. 9). Therefore, most of the strain was localised in the depocentre of the Triassic salt found underneath the western part of the Jbel Amsittene and wedging out towards the east. This is coherent with eastwards decreasing strain observed for both the early post-rift and the Alpine shortening phases.

4.3. Regional shortening in other Moroccan sites during anticline growth

Observations within and nearby the Essaouira-Agadir Basin suggest that some of the other salt structures present in the rifted margin may have been originally formed at earlier times than the Tertiary contraction (e.g., Hafid et al., 2006; Bertotti and Gouiza, 2012; Saura et al., 2013; Benvenuti et al., 2017; Moragas et al., 2018; Pichel et al., 2019a). This could be the case of the Tidsi Anticline and the Imi n'Tanout wedge in the Essaouira-Agadir Basin (Fig. 1B), and the Dadès Valley in the Ouarzazate Basin. These structures may have formed similarly to the Jbel Amsittene Anticline, i.e. during an early post-rift shortening phase

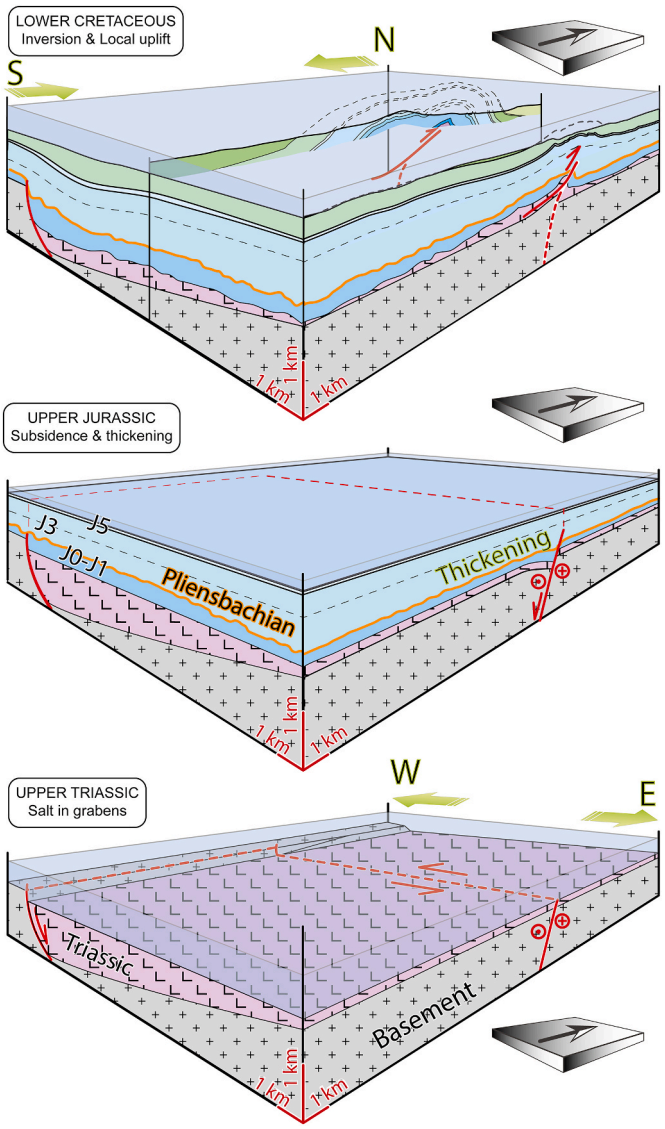

Fig. 9. Evolutionary model of the Jbel Amsittene Anticline. Proposed evolutionary model of the Jbel Amsittene Anticline. In the last time-step we show the anticline with its finite geometry at present, which also results from Alpine tectonism.

that reactivated inherited structures in assistance of the Triassic evaporitic rocks (Fig. 9). However, truncation of the basalt horizons by the Pliensbachian unconformity within certain structures also suggest the presence of earlier salt growth (Hafid et al., 2006).

The Tidsi Anticline, north of the Jbel Amsittene Anticline (Fig. 1B), was also thought to result from salt diapirism during the Late Cretaceous. The main arguments are the presence of growth strata documented in the Upper Cretaceous rocks and the lack of Jurassic series, coupled with the absence of tectonic indicators associated with these growth features (Amrhar, 1995; Hafid, 2006). While the relevance of diapirism in controlling the growth of the Tidsi Anticline during Late Cretaceous time is not unlikely, other older structures are observed in the area which document the existence of Early Cretaceous tectonic deformations hitherto neglected (Bertotti and Gouiza, 2012). This study also documents that the Late Lower Cretaceous strata in the uppermost part of the outcrop are sub-horizontal, which implies deformation occurred prior to the Late Cretaceous. The tectonic nature of these structures is proven by the fold vergence towards the core of the Tidsi Anticline, which is incompatible with an halokinetic origin.

To the east of Jbel Amsittene, the geometry of the post-rift portion of the Imi n'Tanout wedge (Fig. 1B) prior to Alpine shortening has been reconstructed coupling thickness measurements with structural field observations (Zühlke et al., 2004; Bertotti and Gouiza, 2012). These studies show syn-depositional deformation is common in the Imi n'Tanout wedge at the outcrop scale, and folds and thrusts with a NW-SE trending axis are common. These structures document Late Jurassic to Early Cretaceous NE-SW shortening approximately perpendicular to the axis of the Imi n'Tanout wedge suggesting their formation within the same deformation regime. Shortening structures are conformal to the large-scale folds in the northern part of the Essaouira-Agadir Basin that are related to the inversion of the Atlas system.

In the Ouarzazate foreland basin, located ca. 300 km southeast of the Essaouira-Agadir Basin and south of the central High Atlas (Fig. 1A), there is also strong evidence for a pre-Atlasic shortening event (Benvenuti et al., 2017). Observations from the Dadès Valley indicate angular and progressive unconformities of syn-tectonic character within the Middle Jurassic to Lower Cretaceous stratigraphic units (Benvenuti et al., 2017). This study also documents syn-sedimentary tectonic structures that suggests a first Middle Jurassic-Early Cretaceous NNE-SSW to NNW-SSE shortening and a later E-W shortening during the Late Cretaceous (Benvenuti et al., 2017).

4.4. Vertical motion and horizontal deformation during anticline growth

A review of the temporal and spatial distribution of the crustal vertical movements has led to the proposal of an overall exhumation/subsidence history for Morocco and its surroundings (Charton et al., 2018). Present-day basement massifs surrounding the Essaouira-Agadir Basin, i.e. the Anti-Atlas, the Marrakech High Atlas, and the Meseta, have been active sources of sediments throughout the Mesozoic (Fig. 10). Specifically, the Anti-Atlas, south of the Jbel Amsittene area, underwent significant exhumation between the Triassic and Middle Jurassic and during the Late Cretaceous to Present-day, while the Meseta and High Atlas massifs were exhumed from the Middle Jurassic to the Early Cretaceous and towards the end of the Late Cretaceous. This discrepancy in exhumation time led to substantial shifts in source areas, yet to be tested with sedimentary provenance analysis in the Essaouira-Agadir Basin.

Contractional structures in the Cretaceous sedimentary units of the Essaouira-Agadir Basin are coeval with major rearrangements in plate motions related to the opening of the South and North Atlantic Ocean (Fig. 10). Continental separation and accretion of oceanic crust started in the Aptian-Albian time in the South Atlantic (Torsvik et al., 2009), between SW Africa and South America, and in the southern segment of the North Atlantic (Knott et al., 1993; Tucholke et al., 2007), between Iberia and Newfoundland. We propose that the resulting counterclockwise rotation of Africa and the southward drifting of Iberia led to N–S compressive stresses within the African plate. At the same time, the ongoing oceanic accretion and mid-Atlantic ridge push in the Central Atlantic resulted in E-W compressive stresses (e.g., Gouiza et al., 2019). Similarly, another Mesozoic failed rift system between northwest and southern Africa along the Atlantic margin was active in the Early Cretaceous (e.g., Guiraud and Maurin, 1992) that may have triggered N–S far-field stresses in Morocco.

The steady acceleration of the Atlantic Mid-Oceanic ridge spreading during the Jurassic period is a known active process in the Central-Atlantic region that may lead to tectonic stresses (Fig. 10C; Labails et al., 2010). Several drivers may have contributed to the Jurassic erosional exhumation: (a) relatively low sea level (e.g., Snedden and Liu, 2010); (b) far-field intraplate stresses by Mid Oceanic Ridge push; (c) positive dynamic topography (up to 100 m of surface uplift; Barnett-Moore et al., 2017) potentially leading to regional instabilities; (d) high paleo-latitudes (similar to those of the Present-day; after Scotese, 2016, Fig. 10C) and; (e) arid to humid climates in the High Atlas during the Early Jurassic (Wilmsen and Neuweiler, 2007). Some of these processes, or some combination of them, may be responsible for the documented

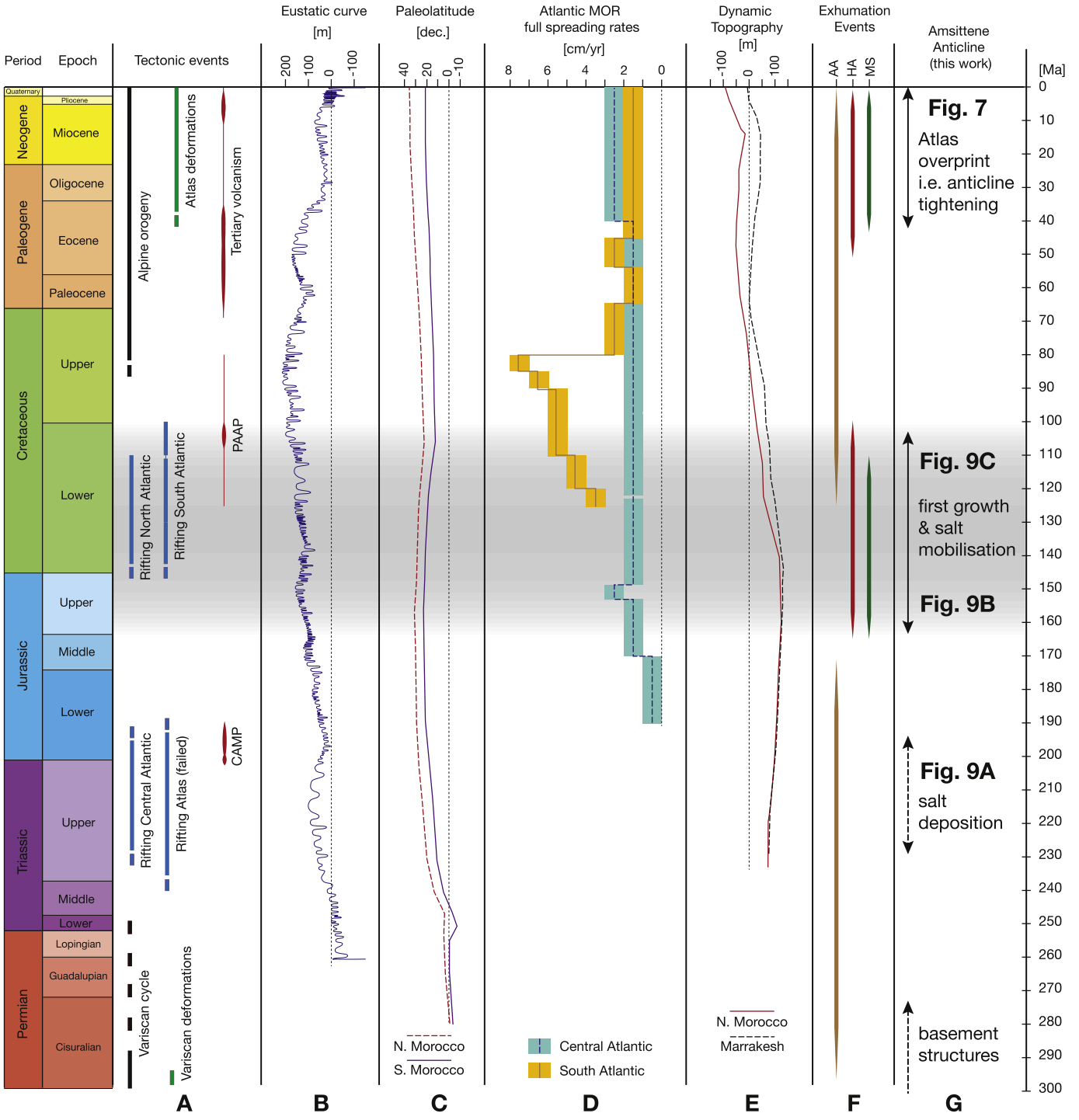

Fig. 10. Time chart and compilation for the Jbel Amsittene Anticline. (A) Tectonic events (Charton, 2018 and the references therein); **(B)** Sea level (Snedden and Liu, 2010); **(C)** Paleolatitude (after maps of Scotese, 2016); **(D)** Full mid oceanic ridge spreading rates (compiled in Charton, 2018); **(E)** Dynamic topography for two points in Morocco (from GPlates website, after model CIs of Barnett-Moore et al. (2017); **(F)** Exhumation events as compiled in Charton (2018); **(G)** Evolution of the Jbel Amsittene (this work). CAMP; Central Atlantic Magmatic Province; PAAP: Peri-Atlantic Alkaline Pulse.

exhumation, and could have resulted in the instability and mobilisation of the Triassic salt by erosion of the sedimentary cap, generating hydraulic heads, or the propagation of faults in the salt cap generated by far-field intraplate stresses and/or surface uplift.

The spatial and temporal relation between these contractional structures and the regional uplift event that affected the NW African margin suggest a common genetic process (Ghorbal et al., 2008; Leprêtre et al., 2015b; Gouiza et al., 2017; Charton et al., 2018). We consider that Late Jurassic-Early Cretaceous shortening in the Essaouira-Agadir Basin was driven by these N–S and E-W compressive stresses that reactivated the E-W (High Atlas/Tethysian failed rift) and N–S (Central Atlantic rift) syn-rift structures alike, and later initiated subsequent salt movements onshore and offshore the Moroccan rifted margin (Hafid et al., 2006; Hafid, 2000, 2006; Tari et al., 2003).

5. Conclusions

We collected detailed structural evidence in the Jbel Amsittene. Our data indicate that the structure is an asymmetrical and north-verging anticline, with a northern flank that dips steeply and locally overturns, and a southern flank that dips south more gently. Our data suggest that the Jbel Amsittene Anticline is a fault-propagation-fold with its detachment plane rooted in Late Triassic evaporites, and that it initially grew during NNW-SSE shortening by the end of the Late Jurassic. Shortening led to anticline-scale and outcrop-scale syn-tectonic wedges in Late Jurassic and Early Cretaceous strata and outcrop-scale syn-sedimentary structures indicating compressional stresses. The anticline lacks structures related to diapiric rise at relevant scales and the effect of salt diapirism is restricted locally to an area around the anticline core. We therefore conclude that the initial development of Jbel Amsittene Ancline during Late Jurassic-Early Cretaceous times was mainly driven by shortening led by compressional tectonics, and only partially the result of salt tectonics. Later inversion of the Atlas system since the Late Cretaceous caused the tightening of the anticline. Being one of many contemporaneous contractional structures reported in the Essaouira-Agadir Basin and nearby basins linked to crustal-scale Middle Jurassic to Early Cretaceous exhumation, our observations suggest a tectonic evolution driven by intraplate stresses along the entire NW African margin.

CRediT authorship contribution statement

D. Fernández-Blanco: Conceptualization, Data curation, Formal analysis, Investigation, Methodology, Project administration, Visualization, Writing - original draft, Writing - review & editing. **M. Gouiza:** Conceptualization, Validation, Visualization, Writing - review & editing. **R. Charton:** Methodology, Validation, Visualization, Writing - review & editing. **C. Kluge:** Methodology, Validation, Visualization, Writing - review & editing. **J. Klaver:** Data curation, Formal analysis, Investigation, Methodology, Visualization. **K. Brautigam:** Data curation, Formal analysis, Investigation, Methodology, Visualization. **G. Bertotti:** Conceptualization, Funding acquisition, Project administration, Resources, Supervision, Validation, Writing - review & editing.

Declaration of competing interest

The authors declare that they have no known competing financial interests or personal relationships that could have appeared to influence the work reported in this paper.

Acknowledgements

Authors would like to thank the careful reviews by two anonymous colleagues on a previous version of the manuscript. DFB wants to thank the Vrije Universiteit Amsterdam for funds that partially covered field-work expenses of this work, part of his M.Sc. Thesis.

Appendix A. Supplementary data

Supplementary data to this article can be found online at https://doi.org/10.1016/j.jsg.2020.104125.

References

Amrhar, M., 1995. Évolution structurale du Haut Atlas Occidental dans le cadre de l'ouverture de l'Atlantique centrale et de la collision Afrique–Europe: Structure, instabilités tectoniques et magmatisme. Thèse Doct. Etat, Univ. Cadi Ayyad, Marrakech.

Barnett-Moore, N., Hassan, R., Müller, R.D., Williams, S.E., Flament, N., 2017. Dynamic topography and eustasy controlled the paleogeographic evolution of northern Africa since the mid-Cretaceous: dynamics topography in northern Africa. Tectonics 36, 929–944.

Bennison, G., Moseley, K., 2004. An Introduction to Geological Structures and Maps, 7ed. Routledge, London. https://doi.org/10.4324/9780203783788.

Benvenuti, M., Moratti, G., Algouti, A., 2017. Stratigraphic and structural revision of the upper mesozoic succession of the Dadès Valley, eastern ouarzazate basin (Morocco). J. Afr. Earth Sci. 135, 54–71.

Bertotti, G., Gouiza, M., 2012. Post-rift vertical movements and horizontal deformations in the eastern margin of the Central Atlantic: middle Jurassic to Early Cretaceous evolution of Morocco. Int. J. Earth Sci. 101, 2151–2165.

Bonow, J.M., Japsen, P., Green, P.F., Cobbold, P.R., Pedreira, A.J., Lilletveit, R., Chiossi, D., 2009. Post-rift landscape development of north-east Brazil. Geol. Surv. Den. Greenl. Bull. 17, 81–84.

Brautigam, K., Fernández-Blanco, D., Klaver, J.M., 2009. Late Jurassic−Early cretaceous horizontal tectonics drives the Jbel Amsittene Anticline in the haha basin, Morocco. In: Master of Science Thesis. Vrije Universiteit Amsterdam.

Charton, R., Bertotti, G., Arantegui, A., Bulot, L., 2018. The Sidi Ifni transect across the rifted margin of Morocco (Central Atlantic): vertical movements constrained by low-temperature thermochronology. J. Afr. Earth Sci. 141, 22–32.

Charton, R.J.G., 2018. Phanerozoic Vertical Movements in Morocco. Delft University of Technology, p. 165. https://doi.org/10.4233/UUID:FDA35870-18D9-4CA3-9443-199A1DCB0250.

Choubert, G., Union Internationale Pour L'étude du Quaternaire, 1965. Evolution de la connaissance du Quaternaire au Maroc. Service Géologique du Maroc.

Duffaud, F., Brun, L., Plauchut, B., 1966. Le bassin du Sud-Ouest marocain. Bassins Sédimentaires Du Littoral Africain. Publ. Assoc. Serv. Géol. Afric 1, 5–26.

Duval-Arnould, A., 2019. Controls on Stratigraphic Development of Shelf Margin Carbonates: Jurassic Atlantic Margin - Essaouira-Agadir Basin, Western Morocco. Doctoral Thesis. Manchester University.

Ellero, A., Malusà, M.G., Ottria, G., Ouanaimi, H., Froitzheim, N., 2020. Transpressional structuring of the high Atlas belt, Morocco. J. Struct. Geol. 135, 104021.

Ellouz, N., Patriat, M., Gaulier, J.-M., Bouatmani, R., Sabounji, S., 2003. From rifting to Alpine inversion: Mesozoic and Cenozoic subsidence history of some Moroccan basins. Sediment. Geol. 156, 185–212.

Frizon de Lamotte, D., 2005. About the cenozoic inversion of the Atlas domain in north Africa. Compt. Rendus Geosci. 337, 475–476.

Frizon de Lamotte, D., Andrieux, J., Guezou, J.C., 1991. Cinematique des chevauchements neogenes dans l'Arc betico-rifain; discussion sur les modeles geodynamiques. Bull. Soc. Geol. Fr. 162, 611–626.

Frizon de Lamotte, D., Saint Bezar, B., Bracène, R., Mercier, E., 2000. The two main steps of the Atlas building and geodynamics of the western Mediterranean. Tectonics 19, 740–761.

Frizon de Lamotte, D., Zizi, M., Missenard, Y., Hafid, M., El-Azzouzi, M., Maury, R.C., Charrière, A., Taki, Z., Benammi, M., Michard, A., 2008. The Atlas system. In: Michard, A., Saddiqi, O., Chalouan, A., de Lamotte, D.F. (Eds.), Continental Evolution: the Geology of Morocco, Lecture Notes in Earth Sciences. Springer Nature, Berlin Heidelberg, pp. 133–202.

Ghorbal, B., 2009. Mesozoic to Quaternary Thermo-Tectonic Evolution of Morocco (NW Africa). Vrije Universiteit Amsterdam.

Ghorbal, B., Bertotti, G., Foeken, J., Andriessen, P., 2008. Unexpected Jurassic to Neogene vertical movements in "stable" parts of NW Africa revealed by low temperature geochronology. Terra. Nova 20, 355–363.

Giles, K.A., Lawton, T.F., 2002. Halokinetic sequence stratigraphy adjacent to the el papalote diapir, northeastern Mexico. AAPG Bull. 86, 823–840.

Gouiza, M., 2011. Mesozoic Source-To-Sink Systems in NW Africa:: Geology of Vertical Movements during the Birth and Growth of the Moroccan Rifted Margin. Vrije Universiteit Amsterdam.

Gouiza, M., Bertotti, G., Charton, R., Haimoudane, K., Dunkl, I., Anczkiewicz, A.A., 2019. New evidence of "anomalous" vertical movements along the hinterland of the Atlantic NW african margin. J. Geophys. Res. https://doi.org/10.1029/2019JB017914 [Solid Earth].

Gouiza, M., Charton, R., Bertotti, G., Andriessen, P., Storms, J.E.A., 2017. Post-Variscan evolution of the Anti-Atlas belt of Morocco constrained from low-temperature geochronology. Int. J. Earth Sci. 106, 593–616.

Green, P.F., Japsen, P., Chalmers, J.A., Bonow, J.M., Duddy, I.R., 2018. Post-breakup burial and exhumation of passive continental margins: seven propositions to inform geodynamic models. Gondwana Res. 53, 58–81.

Guiraud, R., Maurin, J.-C., 1992. Early cretaceous rifts of western and central Africa: an overview. Tectonophysics 213, 153–168.

Hafid, M., 2006. Styles structuraux du Haut Atlas de Cap Tafelney et de la partie septentrionale du Haut Atlas Occidental: tectonique salifère et relation entre l'Atlas et l'Atlantique. Notes Mém. Serv. Géol. Maroc 465, 172.

Hafid, M., 2000. Triassic–early Liassic extensional systems and their Tertiary inversion, Essaouira Basin (Morocco). Mar. Petrol. Geol. 17, 409–429.

Hafid, M., Zizi, M., Bally, A.W., Ait Salem, A., 2006. Structural styles of the western onshore and offshore termination of the High Atlas, Morocco. Compt. Rendus Geosci. 338, 50–64.

Hoggard, M.J., White, N., Al-Attar, D., 2016. Global dynamic topography observations reveal limited influence of large-scale mantle flow. Nat. Geosci. 9, 456.

Hollard, H, Choubert, G, Bronner, G, Marchand, J, Sougy, J., 1985. Carte géologique du Maroc, 1:1,000,000. Geological map, Rabat, Morocco.

Jaïdi, S., Bencheqroun, A., Diouri, M., 1970. Carte géologique du Maroc 1:100 000, feuille tamanar. Not. Mém. Serv. Géol. Maroc 201.

Japsen, P., Bonow, J.M., Green, P.F., Chalmers, J.A., Lidmar-Bergström, K., 2009. Formation, uplift and dissection of planation surfaces at passive continental margins – a new approach. Earth Surf. Process. Landforms 34, 683–699.

Japsen, P., Bonow, J.M., Green, P.F., Chalmers, J.A., Lidmar-Bergström, K., 2006. Elevated, passive continental margins: long-term highs or Neogene uplifts? New evidence from West Greenland. Earth Planet Sci. Lett. 248, 330–339.
Japsen, P., Chalmers, J.A., 2000. Neogene uplift and tectonics around the North Atlantic: overview. Global Planet. Change 24, 165–173.
Japsen, P., Chalmers, J.A., Green, P.F., Bonow, J.M., 2012. Elevated, passive continental margins: not rift shoulders, but expressions of episodic, post-rift burial and exhumation. Global Planet. Change 90–91, 73–86.
Klitgord, K.D., Schouten, H., 1986. Plate kinematics of the central Atlantic. Geol. North Am. 1000, 351–378.
Knott, S.D., Burchell, M.T., Jolley, E.J., Fraser, A.J., 1993. Mesozoic to Cenozoic plate reconstructions of the North Atlantic and hydrocarbon plays of the Atlantic margins. In: Petroleum Geology of Northwest Europe: Proceedings of the 4th Conference. Geological Society of London, pp. 953–974.
Labails, Cinthia, Olivet, Jean-Louis, Aslanian, Daniel, Roest, Walter R, 2010. An alternative early opening scenario for the Central Atlantic Ocean. Earth Planet. Sci. Lett. 297 (3), 355–368. https://doi.org/10.1016/j.epsl.2010.06.024.
Lanari, R., Faccenna, C., Fellin, M.G., Essaifi, A., Nahid, A., Medina, F., Youbi, N., 2020a. Tectonic evolution of the western high Atlas of Morocco: oblique convergence, reactivation, and transpression. Tectonics 39, 1459.
Lanari, R., Fellin, M.G., Faccenna, C., Balestrieri, M.L., Pazzaglia, F.J., Youbi, N., Maden, C., 2020b. Exhumation and surface evolution of the western high Atlas and surrounding regions as constrained by low-temperature thermochronology. Tectonics 39, 197.
Laville, E., Piqué, A., 1992. Jurassic penetrative deformation and Cenozoic uplift in the Central High Atlas (Morocco): a tectonic model. structural and orogenic inversions. Geol. Rundsch.: Zeitschrift Fur Allgemeine Geologie 81, 157–170.
Laville, E., Pique, A., Amrhar, M., Charroud, M., 2004. A restatement of the mesozoic atlasic rifting (Morocco). J. Afr. Earth Sci. 38, 145–153.
Leprêtre, R., Missenard, Y., Barbarand, J., Gautheron, C., Saddiqi, O., Pinna-Jamme, R., 2015a. Postrift history of the eastern central Atlantic passive margin: insights from the Saharan region of South Morocco. J. Geophys. Res. 120, 2014JB011549.
Leprêtre, R., Missenard, Y., Saint-Bezar, B., Barbarand, J., Delpech, G., Yans, J., Dekoninck, A., Saddiqi, O., 2015b. The three main steps of the Marrakech High Atlas building in Morocco: structural evidences from the southern foreland, Imini area. J. Afr. Earth Sci. 109, 177–194.
Le Roy, P., Piqué, A., 2001. Triassic–liassic western Moroccan synrift basins in relation to the central atlantic opening. Mar. Geol. 172, 359–381.
Luber, T.L., Bulot, L.G., Redfern, J., Nahim, M., Jeremiah, J., Simmons, M., Bodin, S., Frau, C., Bidgood, M., Masrour, M., 2019. A revised chronostratigraphic framework for the Aptian of the Essaouira-Agadir Basin, a candidate type section for the NW African Atlantic Margin. Cretac. Res. 93, 292–317.
Malusà, M.G., Polino, R., Feroni, A.C., Ellero, A., Ottria, G., Baidder, L., Musumeci, G., 2007. Post-Variscan tectonics in eastern Anti-Atlas (Morocco). Terra. Nova 19, 481–489.
Medina, F., 1995. Syn- and postrift evolution of the El Jadida – Agadir basin (Morocco): constraints for the rifting models of the central Atlantic. Can. J. Earth Sci. 32, 1273–1291.
Michard, A., Saddiqi, O., Chalouan, A., de Lamotte, D.F., 2008. Continental Evolution: the Geology of Morocco: Structure, Stratigraphy, and Tectonics of the Africa-Atlantic-Mediterranean Triple Junction. Springer.
Moragas, M., Vergés, J., Saura, E., Martín-Martín, J.-D., Messager, G., Merino-Tomé, Ó., Suárez-Ruiz, I., Razin, P., Grélaud, C., Malaval, M., Others, 2018. Jurassic rifting to post-rift subsidence analysis in the Central High Atlas and its relation to salt diapirism. Basin Res. 30, 336–362.
Morley, C.K., Crevello, P., Ahmad, Z.H., 1998. Shale tectonics and deformation associated with active diapirism: the Jerudong Anticline, Brunei Darussalam. J. Geol. Soc. 155, 475–490.
Müller, R.D., Hassan, R., Gurnis, M., Flament, N., Williams, S.E., 2018. Dynamic topography of passive continental margins and their hinterlands since the Cretaceous. Gondwana Res. https://doi.org/10.1016/j.gr.2017.04.028.
Neumaier, M., Back, S., Littke, R., Kukla, P.A., Schnabel, M., Reichert, C., 2016. Late cretaceous to cenozoic geodynamic evolution of the atlantic margin offshore Essaouira (Morocco). Basin Res. 28, 712–730.
Ouajhain, B., Daoudi, L., Laduron, D., Rocha, F., Jean, N., 2011. Jurassic clay mineral sedimentation control factors in the Essaouira basin (western high Atlas, Morocco). Geol. Belg.
Oukassou, M., Saddiqi, O., Barbarand, J., Sebti, S., Baidder, L., Michard, A., 2013. Post-Variscan exhumation of the Central Anti-Atlas (Morocco) constrained by zircon and apatite fission-track thermochronology. Terra. Nova 25, 151–159.
Peulvast, J.-P., Claudino Sales, V., Bétard, F., Gunnell, Y., 2008. Low post-Cenomanian denudation depths across the Brazilian Northeast: implications for long-term landscape evolution at a transform continental margin. Global Planet. Change 62, 39–60.
Pichel, L.M., Finch, E., Gawthorpe, R.L., 2019a. The impact of pre-salt rift topography on salt tectonics: a discrete-element modeling approach. Tectonics. https://doi.org/10.1029/2018tc005174.
Pichel, L.M., Huuse, M., Redfern, J., Finch, E., 2019b. The influence of base-salt relief, rift topography and regional events on salt tectonics offshore Morocco. Mar. Petrol. Geol. 103, 87–113.
Piqué, A., Le Roy, P., Amrhar, M., 1998. Transtensive synsedimentary tectonics associated with ocean opening: the Essaouira–Agadir segment of the Moroccan Atlantic margin. J. Geol. Soc. 155, 913–928.
Piqué, A., Tricart, P., Guiraud, R., Laville, E., Bouaziz, S., Amrhar, M., Ouali, R.A., 2002. The mesozoic-cenozoic Atlas belt (north Africa): an overview. Geodin. Acta 15, 185–208.
Poprawski, Y., Basile, C., Agirrezabala, L.M., Jaillard, E., Gaudin, M., Jacquin, T., 2014. Sedimentary and structural record of the Albian growth of the Bakio salt diapir (the Basque Country, northern Spain). Basin Res. 26, 746–766.
Ruiz, G., Sebti, S., Negro, F., Saddiqi, O., Frizon de Lamotte, D., Stockli, D., Foeken, J., Stuart, F., Barbarand, J., Schaer, J.-P., 2011. From central Atlantic continental rift to Neogene uplift–western Anti-Atlas (Morocco). Terra. Nova 23, 35–41.
Saddiqi, O., El Haimer, F.-Z., Michard, A., Barbarand, J., Ruiz, G.M.H., Mansour, E.M., Leturmy, P., Frizon de Lamotte, D., 2009. Apatite fission-track analyses on basement granites from south-western Meseta, Morocco: paleogeographic implications and interpretation of AFT age discrepancies. Tectonophysics 475, 29–37.
Sahabi, M., Aslanian, D., Olivet, J.-L., 2004. Un nouveau point de départ pour l'histoire de l'Atlantique central. Compt. Rendus Geosci. 336, 1041–1052.
Saura, E., Vergés, J., Martín-Martín, J.D., Messager, G., Moragas, M., Razin, P., Grélaud, C., Joussiaume, R., Malaval, M., Homke, S., Hunt, D.W., 2013. Syn- to post-rift diapirism and minibasins of the Central High Atlas (Morocco): the changing face of a mountain belt. J. Geol. Soc. 171, 97–105.
Scotese, C., 2016. PALEOMAP: paleoatlas for GPlates and the paleodataplotter program. https://doi.org/10.1130/abs/2016nc-275387.
Seguret, M., 1972. Étude tectonique des nappes et séries décollées de la partie centrale des Pyrénées. Thesis. Science Univ, Montpellier.
Sehrt, M., 2014. Variscan to Neogene Long-Term Landscape Evolution at the Moroccan Passive Continental Margin (Tarfaya Basin and Western Anti-atlas). https://doi.org/10.11588/heidok.00017463. Heidelberg.
Snedden, J.W., Liu, C., 2010. A compilation of Phanerozoic sea-level change, coastal onlaps and recommended sequence designations. Search Discov. Artic. 40594, 3.
Stets, J., 1992. Mid-jurassic events in the western high Atlas (Morocco). Geol. Rundsch.: Zeitschrift Fur Allgemeine Geologie 81, 69–84.
Tari, G., Molnar, J., Ashton, P., 2003. Examples of salt tectonics from West Africa: a comparative approach. Geol. Soc. Lond. Spec. Publ. 207, 85–104.
Teixell, A., Arboleya, M.-L., Julivert, M., Charroud, M., 2003. Tectonic shortening and topography in the central High Atlas (Morocco). Tectonics 22, 1051.
Torsvik, T.H., Rousse, S., Labails, C., Smethurst, M.A., 2009. A new scheme for the opening of the South Atlantic Ocean and the dissection of an Aptian salt basin. Geophys. J. Int. 177, 1315–1333.
Tucholke, B.E., Sawyer, D.S., Sibuet, J.-C., 2007. Breakup of the newfoundland–iberia rift. Geol. Soc. Lond. Spec. Publ. 282, 9–46.
Westaway, R., Aït Hssaine, A., Demir, T., Beck, A., 2009. Field reconnaissance of the Anti-Atlas coastline, Morocco: fluvial and marine evidence for Late Cenozoic uplift. Global Planet. Change 68, 297–310.
Wilmsen, M., Neuweiler, F., 2007. Biosedimentology of the Early Jurassic post-extinction carbonate depositional system, central High Atlas rift basin, Morocco: early Jurassic biosedimentology. Sedimentology 55, 773–807.
Zühlke, R., Bouaouda, M.-S., Ouajhain, B., Bechstädt, T., Leinfelder, R., 2004. Quantitative meso-/cenozoic development of the eastern central atlantic continental shelf, western high Atlas, Morocco. Mar. Petrol. Geol. 21, 225–276.